EPA/600/A-97/092
For presentation at the American Meteorological Society
10th Joint Conference on the Applications of Air Pollution
Meteorology with the AWMA, Phoenix, AZ Jan. 11 - 16, 1998

9B.3 RECENT EXPERIMENTS ON BUOYANT PLUME DISPERSION IN A LABORATORY CONVECTION TANK

J.C. Weil

CIRES, University of Colorado
Boulder, Colorado

W.H. Snyder

Mechanical Engineering Department, University of Surrey
Guildford, Surrey, England

R.E. Lawson, Jr.*

ASMD, ARL, National Oceanic and Atmospheric Administration
Research Triangle Park, North Carolina

M.S. Shipman

Geophex, Ltd.
Raleigh, North Carolina

1. INTRODUCTION

Buoyant plumes from tall stacks usually produce their highest ground-level concentrations (GLCs) in a convective boundary layer (CBL), where turbulent downdrafts bring elevated plume sections to the surface. Our understanding of buoyant plume dispersal has been significantly advanced by Willis and Deardorff's (1983, 1987) experiments in a laboratory convection tank. Their studies demonstrated the complex dispersion patterns and the dependence of plume properties on the dimensionless buoyancy flux $F_* = F_b/(Uw_*^2 z_i)$, where F_b is the stack buoyancy flux, U is the mean wind speed, w_* is the convective velocity scale, and z_i is the CBL depth. For $F_* = 0.03$, the plume behaved similarly to a nonbuoyant plume after some initial rise, but for $F_* = 0.11$, the plume rose to the CBL top, where it "lofted" or remained temporarily and then gradually mixed downwards. Field observations around tall stacks suggested that the maximum hourly-averaged GLCs generally occur for the lofting situation (e.g., Hanna and Paine, 1989).

In related experiments, Deardorff and Willis (1984) investigated concentration fluctuations for elevated sources and found large near-surface values of the fluctuation intensity σ_c/C (i.e., ≥ 1); here, C is the ensemble-mean concentration and σ_c is the root-mean-square (rms) concentration fluctuation. The σ_c/C decreased significantly with increasing distance along the plume centerline. Later experiments provided much needed information on the probability distribution of the concentration (Deardorff and Willis, 1988).

While clearly revolutionary, these experiments were limited by the measurement techniques and the small sample sizes collected. For example, in the highly-buoyant plume studies, only 4 to 9 repetitions of the concentration profiles were obtained (Willis and Deardorff, 1987). This resulted in uncertainty in the C values near the surface and underestimates of the lateral plume spread σ_y (see later discussion).

The above limitations were overcome in recent convection tank experiments conducted at the EPA Fluid Modeling Facility in North Carolina. The main experimental objective was to obtain statistically-reliable dispersion characteristics including C, σ_c, σ_y, etc. for highly-buoyant plumes, $F_* \geq 0.1$. Since the concentration fluctuations were known to be large, a key design feature was a means for obtaining a sufficiently large number of measurements to ensure such reliability.

2. EXPERIMENT DESCRIPTION

The experimental arrangement was quite similar to that of Willis and Deardorff (1987). The convection tank was about 124 cm on a side, was filled

---

* On assignment to NERL, U.S. Environmental Protection Agency.

Corresponding author address: J.C. Weil, NCAR, P.O. Box 3000, Boulder, CO 80307

with water to a depth of 34 cm, and had an initial stratification aloft of 1°C/cm. The convection was driven by an electrically-heated bottom surface that produced a $z_i \simeq 20$ cm and $w_* = 0.74$ cm/s at the time of the measurements. A mean wind was simulated by towing a model stack (height $z_s = 3$ cm) along the tank floor at a speed U of 2.07 cm/s. The stack emitted a water - ethanol mixture to simulate the buoyancy, and the mixture contained a small amount of Rhodamine dye, which fluoresced when excited by laser light.

In an approach different from that of Willis and Deardorff, a laser was mounted on a movable table alongside the tank and towed at the stack speed in order to illuminate a y - z (crosswind, vertical) plane at a fixed distance x downstream of the stack. Pictures of the fluorescent dye were taken from a camera viewing this plane end-on; the light intensity was digitized, stored, and subsequently converted to concentration in y and z intervals of 0.2 cm. In each tow, 59 cross-sectional images were digitally recorded (at 0.8 s intervals) as the stack traversed the tank. The tow was repeated 6 - 7 times for a total of 354 - 413 realizations of each cross section. This is an unprecedented data volume.

Four experiments were performed each with a different F_* but the same effluent speed, U, and CBL variables; the F_* values were 0, 0.1, 0.2 and 0.4, with $F_* = 0$ serving as a reference case. In each experiment, 8 downwind cross sections were sampled.

3. RESULTS

We present salient features of the horizontal scalar flux, plume spatial statistics, and concentration fields. We use convective scaling of dispersion wherein z_i and w_* are the relevant turbulence length and velocity scales (Willis and Deardorff, 1987). An appropriate dimensionless distance is

$$X = w_* x/(U z_i) \ , \tag{1}$$

which is the ratio of travel time x/U to the convective time scale z_i/w_*.

The horizontal scalar flux Γ in each sampled cross section was determined from

$$\Gamma = \int\int c(x, y, z) U dy dz \ , \tag{2}$$

where c is the "instantaneous" concentration. Figure 1a shows an example pseudo time-series of the ratio Γ/Q, where Q is the source flux. The above was constructed by arranging the measurements from 7 tows in a time sequence using the sampling interval (0.8 s). As can be seen, there is a large variability in Γ/Q—from 0.1 to ~ 3, although on average, the mean flux $\overline{\Gamma} = Q$. We believe that the variability is caused by longitudinal velocity fluctuations and by the convergence/divergence of the flow at the boundaries, i.e., the exchange of fluid and scalar from updrafts to downdrafts and vice versa at $z = 0$ and z_i.

In each of the four experiments, the $\overline{\Gamma}$ averaged over the 8 downwind distances was within 20% of Q. As a correction to c, we multiplied the c in all realizations by the inverse of the initial average

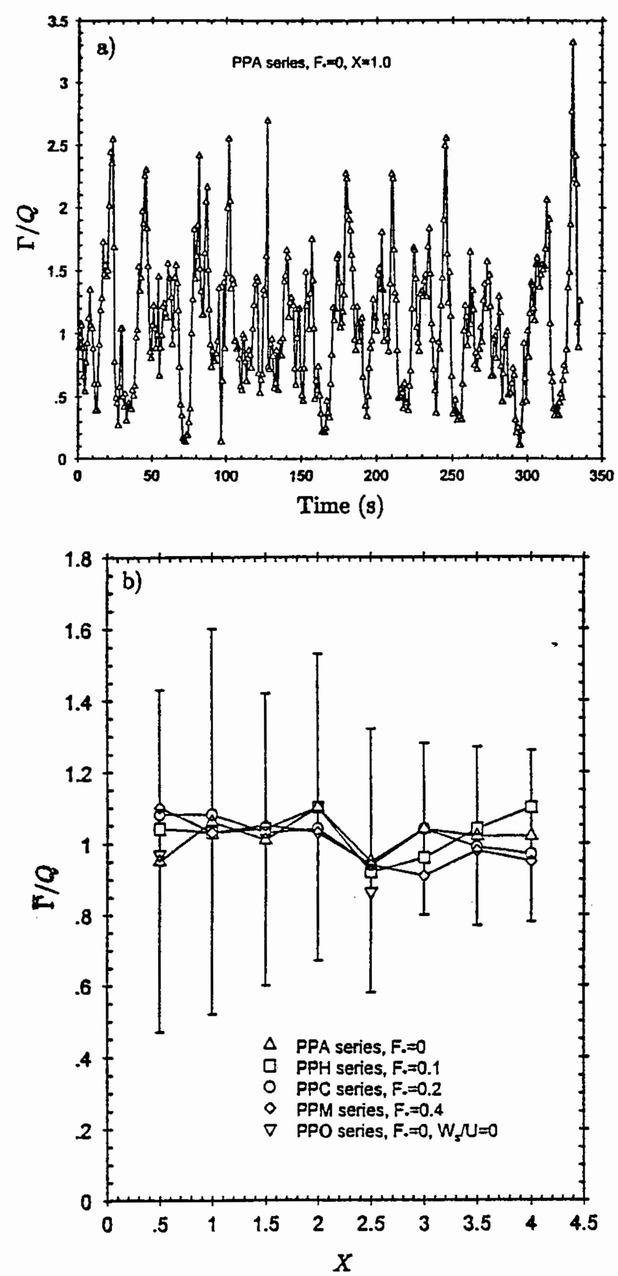

Fig. 1. a) Time series of plume horizontal scalar flux, and b) mean scalar flux as a function of dimensionless distance X.

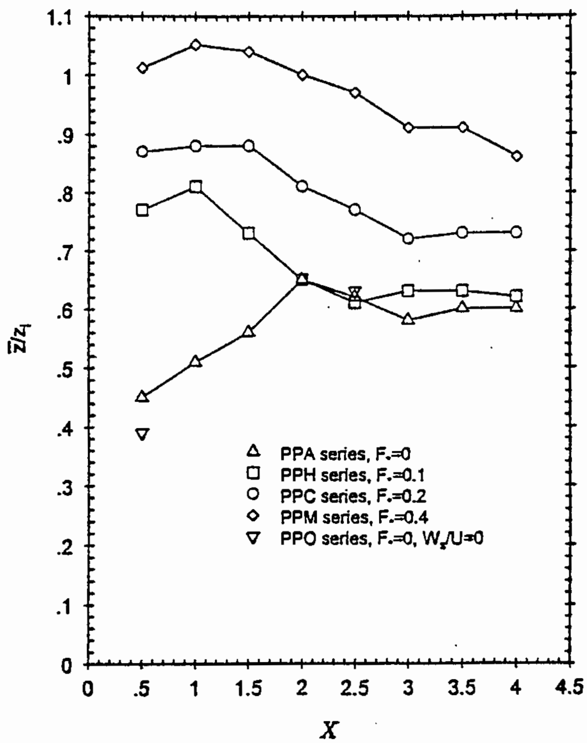

Fig. 2. Dimensionless mean plume height versus X.

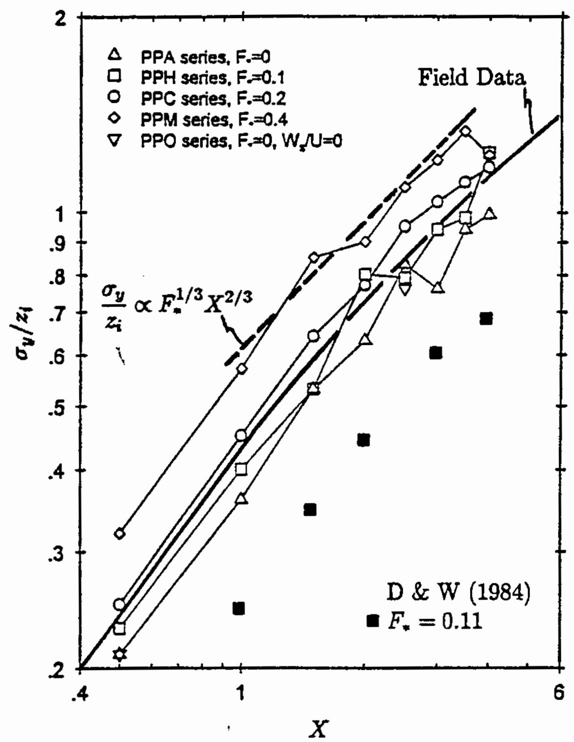

Fig. 3. Dimensionless crosswind dispersion as a function of X.

flux ratio ($\overline{\Gamma}/Q$) for each experiment. Figure 1b presents the variation of the "corrected" $\overline{\Gamma}/Q$ with X and demonstrates that it is within 10% of the ideal value 1 at each X. The rms deviation (bars) for $F_* = 0$ (PPA series) shows that it is greatest near the source and diminishes far downstream due to the greater homogenization of the scalar; a similar rms behavior is found for the other cases. In contrast to the above, Willis and Deardorff (1987) and Deardorff and Willis (1988) used a correction to c that ranged from 1/3 to 3.

Figure 2 shows that the dimensionless mean plume height $\overline{z}/z_i$ varies systematically with both F_* and X. Note that for $F_* = 0.1$ and $X < 2$, the buoyancy has a profound effect in increasing $\overline{z}$ relative to the nonbuoyant case (PPA), but for $X \geq 2$, the $\overline{z}$'s for these two cases are quite close. At $X = 4$, the $\overline{z}/z_i$ for the two cases is $\simeq 0.6$ instead of the expected 0.5 for a uniformly-mixed plume below z_i. Our result is consistent with the vertical profile of the crosswind-integrated concentration (CWIC) for $F_* = 0$, which exhibits a well-mixed distribution for $z/z_i \leq 1.15$. More recent measurements show that the well-mixed depth is perhaps 5 to 10% lower. Thus, there is some uncertainty in the final equilibrium $\overline{z}$ values, and this is under investigation.

Figure 3 presents new measurements (open symbols) of the dimensionless crosswind dispersion σ_y/z_i as a function of X and displays several features: 1) the σ_y/z_i for $F_* = 0$ to 0.2 is in reasonable agreement with the mean σ_y/z_i deduced from field observations of buoyant plumes (heavy solid curve; Weil and Corio, 1985), 2) the new data are more consistent with the field observations than are the Deardorff and Willis (D & W, 1984) results which are only 60% as large, and 3) the new measurements show that σ_y is slightly enhanced for $F_* = 0.2$, relative to the $F_* = 0$ and 0.1 cases, and clearly enhanced for $F_* = 0.4$ as suggested by field observations of highly-buoyant plumes ($F_* > 0.1$; Briggs, 1985). Briggs' expression is $\sigma_y/z_i = a_1 F_*^{1/3} X^{2/3}$ with $a_1 = 1.6$. The tank data show that this functional dependence is followed (dashed line) but that the coefficient a_1 (= 0.47) is only 30% of the field value. This may be partially explained by other effects (crosswind shear, mesoscale variability, etc.) that are present in the field but absent in the convection tank.

From the repeated cross section measurements, we determined the spatial distributions of C, σ_c, and the CWIC $C^y = \int_{-\infty}^{\infty} C(x,y,z)dy$. Figure 4 gives an example of the dimensionless CWIC $C^y U z_i/Q$ as a function of z/z_i and X for $F_* = 0.2$. This clearly shows the maintenance of an elevated maximum in C^y above z_i and the C^y profile development within the mixed layer ($z < z_i$) over the range $X < 3$. For $X \geq 3$, the profile below

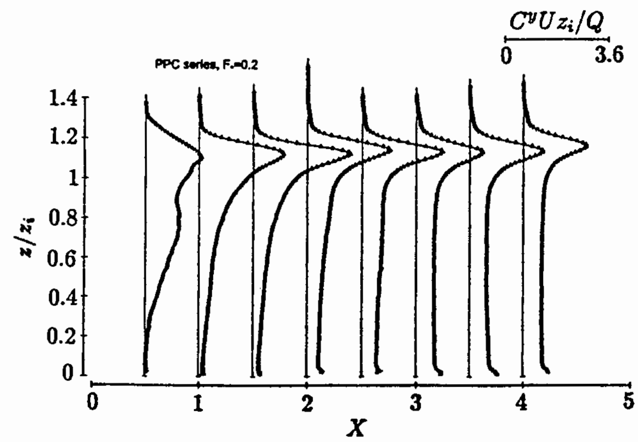

Fig. 4. Vertical profiles of C^yUz_i/Q versus X.

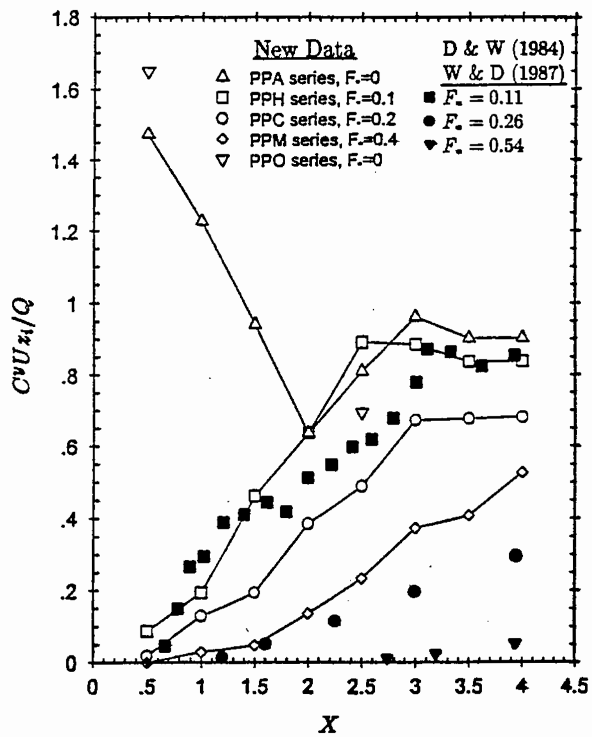

Fig. 5. Surface value of C^yUz_i/Q as a function of X.

z_i is essentially uniform but with a magnitude less than the well-mixed value, $C^yUz_i/Q = 1$. For $X > 4$, we expect that the elevated maximum C^y would diminish and the CWIC in the mixed layer would increase due to entrainment of the plume aloft. The maintenance of the elevated maximum near its initial height ($\overline{z}/z_i \simeq 1.1$) differs from the Willis and Deardorff (1987) observations, which

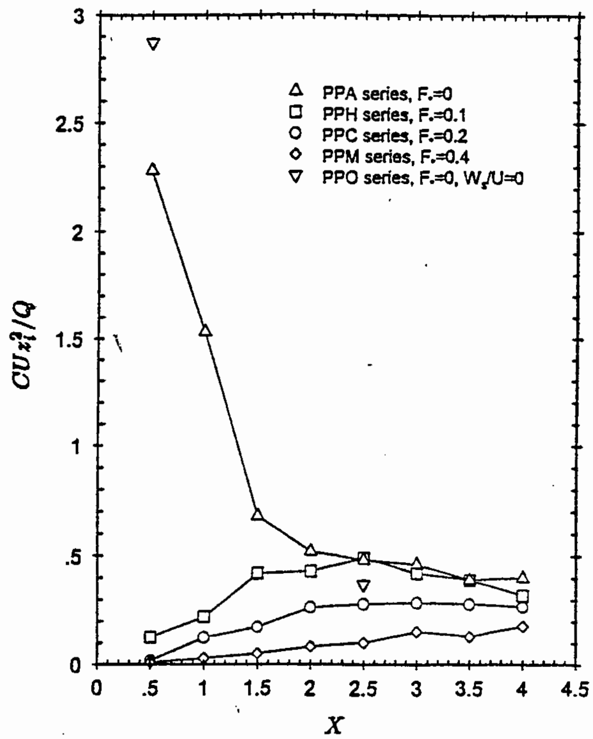

Fig. 6. Dimensionless ground-level concentration versus X.

showed the maximum C^y first to overshoot z_i and then to remain at or below z_i as X increased.

The dimensionless CWIC near the surface (Fig. 5) shows that the addition of buoyancy significantly reduces the CWIC near the source ($X < 2$) by comparison to the nonbuoyant case (PPA). For $X \geq 2$, the moderately-buoyant case ($F_* = 0.1$, PPH) follows the nonbuoyant case rather well as also found for $\overline{z}/z_i$. Further systematic reductions in the CWIC result as F_* increases from 0.1 to 0.4, a trend also found by Willis and Deardorff (W & D, 1987). However, as seen in Fig. 5, their results are lower than ours, especially for $F_* > 0.1$. This may be due to insufficient repetitions in their experiments as suggested by their paper.

For dispersion applications, the quantity of most interest is the surface concentration which is displayed in dimensionless form in Fig. 6; the concentration is along $y = 0$ and $z/z_i = 0.05$. Again, we observe that the buoyancy has a dramatic effect in reducing the near-source concentrations. The concentrations for $F_* = 0$ and 0.1 are approximately the same for $X > 2.5$ due to the plume becoming vertically well-mixed and to the similarity in their σ_y values (Fig. 3).

Figure 7 shows the near-surface values of σ_c/C (along $y = 0$) as a function of X and F_*. At $X = 0.5$, the data clearly demonstrate a systematic increase in σ_c/C with F_*, a result not previously

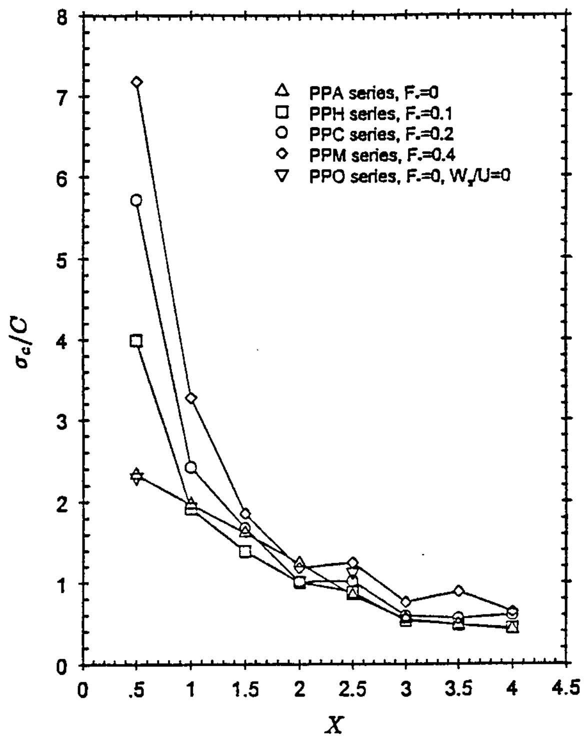

Fig. 7. Concentration fluctuation intensity at the surface versus X.

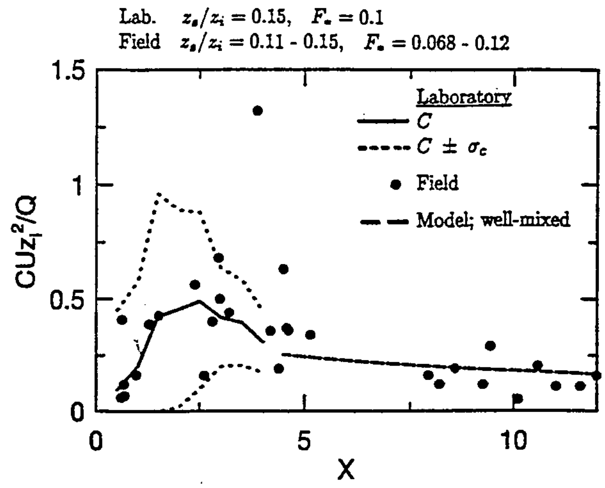

Fig. 8. Dimensionless ground-level concentration distribution for laboratory and field data.

attained. This behavior is due to the increasingly elevated plume centerlines for the more buoyant releases (Fig. 2), and hence to a more intermittent plume at the surface. Although there is a significant variation with F_* at short range, the σ_c/C exhibits a more gradual variation with X for $X > 1.5$ and collapses to a nearly universal distribution. This is attributed to the greater homogenization of the plume within the mixed layer as X increases.

To test the laboratory results, we compared the centerline GLCs (i.e., along $y = 0$) with field observations downwind of the Kincaid power plant. The plant had a 187-m stack and emitted an SF_6 tracer during an intensive field program (Hanna and Paine, 1989). The data used here are the maximum 1-hr SF_6 GLCs on crosswind arcs, which ranged from 1.2 to 30 km downwind. The meteorological variables had the following values: $1124\ \text{m} \leq z_i \leq 1750\ \text{m}$, $2.4\ \text{m/s} \leq U \leq 4.5\ \text{m/s}$, and $2.0\ \text{m/s} \leq w_* \leq 2.6\ \text{m/s}$.

Figure 8 compares the dimensionless GLC CUz_i^2/Q from the laboratory and field, where the field values of z_s/z_i and F_* are close to their laboratory counterparts of 0.15 and 0.1, respectively. We believe that the agreement between the two data sets is quite good considering the vast difference in scale and the absence of extraneous effects (mesoscale variability, etc.) in the convection tank. Figure 8 also presents a model result based on a vertically well-mixed scalar distribution with $CUz_i^2/Q = 1/[(2\pi)^{1/2}\sigma_y/z_i]$; we have adopted $\sigma_y/z_i = 0.56X/(1 + 0.7X)^{1/2}$ (Weil and Corio, 1985). This modeled GLC (dashed line) is an adequate fit for $X > 5$. Note that for $X \leq 4$, nearly all of the field observations are within $\pm\sigma_c$ of the laboratory C, and the field data variability is greatest in this region as the laboratory data suggest.

4. CONCLUDING REMARKS

New convection tank experiments on buoyant plume dispersion have been performed with F_* ranging from 0 to 0.4. The main objective of obtaining statistically-reliable dispersion characteristics—C, σ_c, σ_y, etc.—was fulfilled. Some results (e.g., the surface CWIC) showed trends similar to those found earlier by Willis and Deardorff (1987), but our results also exhibited some notable differences from and advancements over the earlier data. For example, the new data showed the: 1) σ_y agreement with field data and enhancement due to plume buoyancy for $F_* > 0.1$, 2) surface C and σ_c/C variation with X, and 3) agreement between the centerline GLC distribution and field observations. This new experimental data base will be of considerable value in future model development efforts. Further experiments over a greater range of z_s/z_i and for other F_* values also would be of much benefit.

5. ACKNOWLEDGMENTS

We are grateful to Jie Lu for assistance in the experimental design and to David Miller and G. Leonard Marsh for help in the data collection and analysis. This work was supported by the DOD/DOE Strategic Environmental Research and Development Program through a Cooperative Agreement between the U.S. EPA and The Pennsylvania State University with a subcontract to the University of Colorado.

6. DISCLAIMER

This paper has been reviewed in accordance with the U.S. Environmental Protection Agency's peer and administrative review policies and approved for presentation and publication. Mention of trade names or commercial products does not constitute endorsement or recommendation for use.

7. REFERENCES

Briggs, G.A., 1985: Analytical parameterizations of diffusion: the convective boundary layer. *J. Climate Appl. Meteor.*, **24**, 1167–1186.

Deardorff, J.W., and G.E. Willis, 1984: Ground-level concentration fluctuations from a buoyant and a non-buoyant source within a laboratory convectively mixed layer. *Atmos. Environ.*, **18**, 1297–1309.

Deardorff, J.W., and G.E. Willis, 1988: Concentration fluctuations within a laboratory convectively mixed layer. *Lectures on Air Pollution Modeling*, A. Venkatram and J.C. Wyngaard, Eds., Amer. Meteor. Soc., Boston, 357–384.

Hanna, S.R., and R.J. Paine, 1989: Hybrid plume dispersion model (HPDM) development and evaluation. *J. Appl. Meteor.*, **28**, 206–224.

Weil, J.C., and L.A. Corio, 1985: Dispersion formulations based on convective scaling. Maryland Power Plant Siting Program, Maryland Dept. of Natural Resources, Annapolis, MD, Rept. No. PPSP-MP-60.

Willis, G.E., and J.W. Deardorff, 1983: On plume rise within the convective boundary layer. *Atmos. Environ.*, **17**, 2435–2447.

Willis, G.E., and J.W. Deardorff, 1987: Buoyant plume dispersion and inversion entrapment in and above a laboratory mixed layer. *Atmos. Environ.*, **21**, 1725–1735.

TECHNICAL REPORT DATA

1. REPORT NO.	2.	3.
EPA/600/A-97/092		

4. TITLE AND SUBTITLE	5. REPORT DATE
Recent Experiments on Buoyant Plume Dispersion in a Laboratory Convection Tank	
	6. PERFORMING ORGANIZATION CODE

7. AUTHOR(S)	8. PERFORMING ORGANIZATION REPORT NO.
[1]Weil, J.C., [2]W.H. Snyder, [3]R.E. Lawson, Jr., and [4]M.S. Shipman	

9. PERFORMING ORGANIZATION NAME AND ADDRESS	10. PROGRAM ELEMENT NO.
[1]CIRES, University of Colorado Boulder, CO	
[2]Mechanical Engineering Depaartment, University of Surrey Guilford, Surrey, England	11. CONTRACT/GRANT NO.
[3]Same as Block 12	
[4]Geophex, Ltd. Raleigh, NC	

12. SPONSORING AGENCY NAME AND ADDRESS	13. TYPE OF REPORT AND PERIOD COVERED
National Exposure Research Laboratory Office of Research and Development U.S. Environmental Protection Agency Research Triangle Park, NC 27711	14. SPONSORING AGENCY CODE EPA/600/9

15. SUPPLEMENTARY NOTES

16. ABSTRACT

Buoyant plumes from tall stacks usually produce their highest ground-level concentrations (GLCs) in a convective boundary layer (CBL), where turbulent downdrafts bring elevated plume sections to the surface. Our understanding of buoyant plume dispersal has been significantly advanced by Willis and Deardorff's (1983, 1987) experiments in a laboratory convection tank. Their studies demonstrated the complex dispersion patterns and the dependence of plume properties on the dimensionless buoyancy flux $=F_b/(Uw_*$, where F_b is the stack buoyancy flux, U is the mean wind speed, w_* is the convective velocity scale, and z_i is the CBL depth. For $F_* = 0.03$, the plume behaved similarly to a nonbuoyant plume after some initial rise, but for $F_* = 0.11$, the plume rose to the CBL top, where it "lofted" or remained temporarily and then gradually mixed downwards. Field observations around tall stacks suggested that the maximum hourly-averaged GLCs generally occur for the lofting situation (e.g., Hanna and Paine, 1989).

17. KEY WORDS AND DOCUMENT ANALYSIS

a. DESCRIPTORS	b. IDENTIFIERS/ OPEN ENDED TERMS	c. COSATI

18. DISTRIBUTION STATEMENT	19. SECURITY CLASS *(This Report)*	21. NO. OF PAGES
	20. SECURITY CLASS *(This Page)*	22. PRICE